A Method for Linearization of Optically Insulated Voltage Transducers

DANIELE GALLO[1], CARMINE LANDI[1], MARIO LUISO[1],
EDOARDO FIORUCCI[2], GIOVANNI BUCCI[2], FABRIZIO CIANCETTA[2]

[1]Department of Information Engineering
Second University of Naples
Via Roma 29 - 81031 Aversa (CE),
ITALY
daniele.gallo@unina2.it, carmine.landi@unina2.it, mario.luiso@unina2.it

[2]Department of Electrical and Information Engineering
University of L'Aquila
Via G. Gronchi 18 – Pile, 67100 L'Aquila
ITALY
giovanni.bucci@univaq.it, edoardo.fiorucci@univaq.it, fabrizio.ciancetta@univaq.it

Abstract: - In the perspective of a capillary power system monitoring, measurement transducers must have larger and larger bandwidth and accuracy, due to proliferation on power grids of new power quality phenomena. Various types of voltage transducers, based on different operation principles, have been realized; in particular, those based on voltage dividers and optical insulation with digital communication seem to offer suitable features for an accurate disturbance monitoring. Anyway, very often they present high cost, too, and so this strongly limit their diffusion. Optical insulation with analog communication could offer all the desired features: nevertheless it is obtained through non-linear devices. So, in this paper a low cost method for linearization of voltage transducers for power systems, based on an optical insulation with analog communication, is presented. The described method is used to implement a prototype of a voltage transducer, whose design, simulation and realization are presented. Experimental characterization has shown that, despite the low cost, the transducer has very good performance, in terms of accuracy, bandwidth and linearity.

Key-Words: - transducers, voltage measurement, power system measurement, power quality, frequency response, linearization.

1 Introduction

As the power electronics advance and renewables proliferate on power grids, conducted disturbances increasingly pollute electrical networks and they grow in amplitude and frequency. As an instrument is intended for power and power quality measurements, it must fulfill recommendations of international standards about quality of electricity supplied by public distribution systems [1]-[2]. The trends of such international standards is to extend the upper corner of the bandwidth of disturbances to be measured, as compatibility levels in industrial plants for conducted disturbances have to be defined in an increasing frequency range. Therefore commercial instrumentation has to face the issue of monitoring the quality of energy over an increasing frequency range; it is also well known that the first part of a power quality measurement chain are voltage and current transducers. Another important parameter, that a measuring instrumentation must guarantee, is the galvanic insulation, in order to preserve safety of operators.

Typical voltage and current measurement transformers, although they are the most installed transducers in the utility points, since they have good insulation characteristics, are typically usable in the narrow 50-400 Hz frequency range. Obviously those limits make them unusable for the analyses of high frequency harmonic and of low frequency interharmonic components.

Other kinds of voltage transducers have been developed and they are based on various operation principles ([6]-[13]). Particularly, some of them ([6], [7], [10]-[13]) obtain galvanic insulation by means of an optical transmission link between input and output sections of the transducer: they all utilize the optical link to transmit information in a digital form. Some of the cited papers present realizations

of voltage transducers with good accuracy and bandwidth: anyway they are characterized also by not so low cost. Also the authors have proposed an approach to develop a low cost optically insulated voltage transducer in [14], [15]; in those papers, the signal at the input stage is digitally converted and transmitted through the optical link as digital information to the output stage.
In this paper a different approach is used: the signal at the input stage is converted to a light signal proportional to it and then transmitted through the optical link as an analog information. Anyway, since the conversion current/light power is not linear, a low cost method for linearization of the optical link is described. Using this new approach a performance improvement can be observed. Moreover the realized prototype solves both the bandwidth limitations and the error problems of the measurement transformers, keeping at the same time their insulation characteristics; it also has a very low cost.
In section II the method for the linearization of the optical insulation stage and in section III the design of the whole voltage transducer are presented. Section IV shows the simulation of the transducer in PSpice environment. Finally, section V deals with experimental tests on the prototype of the realized voltage transducer (RVT), aimed to evaluate its performance, executed through a purpose-made automated measuring station.

2 Method of linearization

As it is well known ([16]), an optical transmitter has a non-linear current/light power characteristic. This fact has forced to use, in power system applications, an optical link as a mean to obtain galvanic insulation only as a digital communication channel. In fact, since a digital communication, either serial or parallel, is composed of a sequence of pulses and the information is only linked to a low or high level of such pulses, even if the channel produces a distortion in the transmitted waveform, the information is preserved. The most important parameter of a digital optical communication channel is the response time, which is in turn inversely proportional to frequency bandwidth: the lower is the response time, the wider is the frequency bandwidth and thus the higher is the baud rate of the channel.
On the contrary, in an analog optical communication channel, since the information is linked to the shape of the transmitted waveform, the distortion must be as low as possible.
The basic idea at the base of this paper comes from control system theory: if a non-linear system is utilized around a working point in a quite linear portion of its characteristic and inserted in a feedback loop control scheme, it can be considered a linear system [17].
For the case in question, the non linear system is the optical transmitter (OT): if it is coupled to an optical receiver (OR), the relationship among input and output currents in non linear, since the relationship among input current and transmitted light power is non linear. A simplified block scheme of this situation is shown in Figure 1.

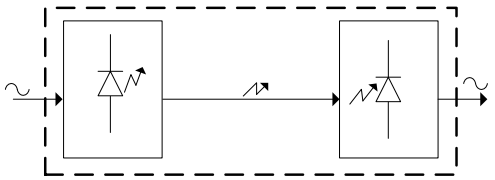

Fig.1 - Block scheme of the open loop optical link

Anyway, if another OR, matched with the first one, is used in a feedback loop control scheme as in Figure 2, its role becomes crucial: it senses the transmitted light power and its output current modifies the current in the OT in order to have a linear relationship among the global output and input currents. It is worthwhile underlining the vital importance of the matching between the two OR: the better the matching is, the more effective the linearization will be.

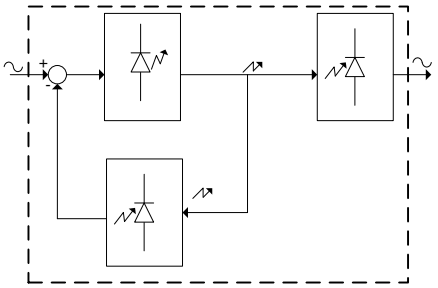

Fig.2 - Block scheme of the closed loop optical link

Therefore, in order to realize a linear analog optical link, a OT and two matched OR have been utilized: they are low cost component, since its cost is about 1 € each one. The characteristics of the OT are: input current in the range of 0÷30 mA, maximum reverse voltage of 9 V, -3 dB frequency bandwidth of 9 MHz.
With the aim of characterizing the open loop current-to-current transfer curves of the couples

OT/OR1 and OT/OR2, an automated measuring station has been made up. It is composed of a PXI platform, three digital multimeters with 6½ digits and resolution of 10 nA, one programmable DC power supply: with it some experimental tests have been performed. First of all, the ratios input/output current, for the two couples, have been found, adopting as reference value a current in the OT of 15 mA: they are equal to 222.38 and 222.48, respectively for the couples OT/OR1 and OT/OR2. Then, current in the OT has been varied in the range of $10\ \mu A \div 30$ mA. In Figure 3.a, the relative deviations of the ratios with respect to their values at 15 mA, are shown, while in Figure 3.b there is a zoom of Figure 3.a. As it can be seen, these relative deviations are very high for low input current values and they are lower than 5 % for input current values higher than 1 mA. Moreover, analyzing the shape of the curves it is clear that there are non linear relationships input/output currents.

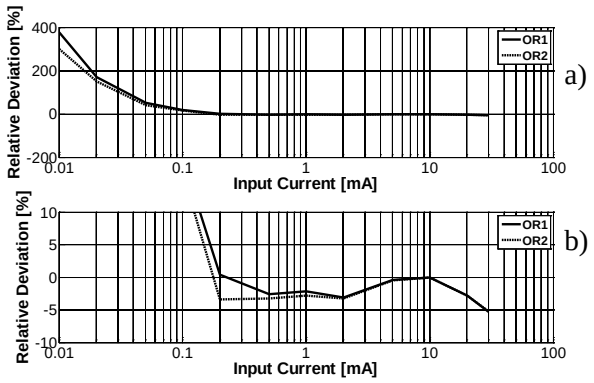

Fig.3 - a) Relative deviations of the ratios input/output currents, for the couples OT/OR1 and OT/OR2, with respect to their values at 15 mA; b) zoom of the a).

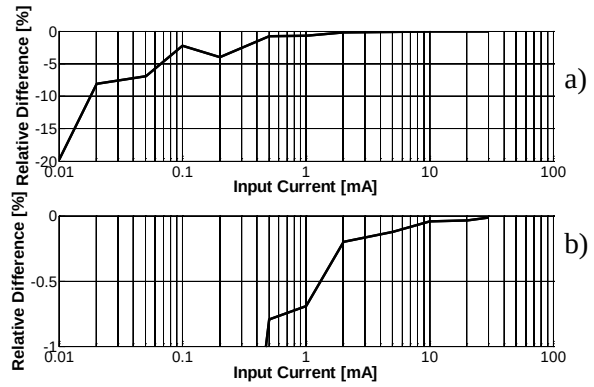

Fig.4 - a) Relative difference of the currents in the two OR, as function of current in the OT; b) zoom of the a).

Figure 4.a shows the relative difference of the currents in the two OR, as function of current in the OT; in Figure 4.b there is a zoom of Figure 4.a. The difference among the two currents is about 20 % at low current values; over 1 mA the difference is under 0.7 % and around 15 mA it is under 0.05 %.
As it will be explained in the next sections, for the realization of the transducer, the OT will be polarized around 15 mA, and thus in a portion of its characteristic where the matching difference among the two OR is very low.
Thanks to this good matching, in the following section it will be shown that the use of the OT and the two OR in closed loop scheme, as in Figure 2, will result in a linear analog communication link.

3 Design of a transducer based on the linearization method

The design of a voltage transducer, intended for power quality measurements, must begin from the analysis of the international standards [1]-[2]. From the analysis of [2] it is evident that the most strict uncertainty level is established for the assessment of the root mean square (r.m.s.) value of the supply voltage, which has to be measured with accuracy of ±0.1 %. Moreover, in [1], which deals with compatibility levels in industrial plants for low-frequency conducted disturbances, limits for voltage components up to 9 kHz are established. It has not to be ignored that this limit is increasing year after year, due to advance in power electronics and switching devices.
A requirement comes once more from [2]: voltage transducers should be sized to prevent measured disturbances from inducing saturation.
This requires that the knee point of the transducer saturation curve be at least 200% of the nominal system voltage. All these considerations results in the following design specifications: a voltage transducer must have accuracy of ±0.1 % at least until 9 kHz and its full scale range must be at least 200% of the nominal system voltage. The RVT has been designed accounting these requirements on accuracy, frequency bandwidth and input full scale range.
The core of the RVT consists of the optical insulation stage. It is made by an OT and an OR, which are optically coupled. The block scheme of the RVT is shown in Figure 5.
Input voltage (V_{IN}) is connected to the first block which is a compensated high impedance voltage divider, made of resistors and capacitors, with an active impedance adaptor. It divides and adapts

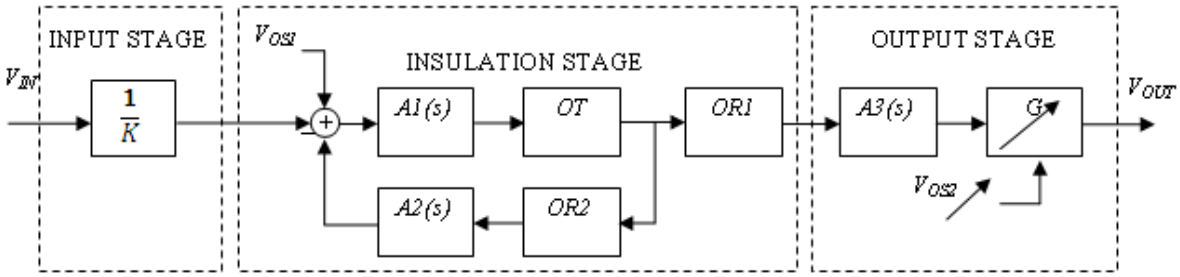

Fig. 5 - Block scheme of the realized voltage transducer

input voltage to make it suitable for successive stages. Its input full scale range, which is the full scale range of the entire RVT, is ±1200 V: this value is about the double of the peak of a line-to-line low voltage level, chosen according the previously described requirement on full scale range. Input voltage is divided by a factor *K* equal to 240: at the input of insulation stage voltage level is in the range of ±5 V.

The insulation stage is used to obtain galvanic insulation between input and output voltages. It is made by one *OT*, two *OR* and two active adaptors *A1(s)* and *A2(s)*. An offset (V_{OS1}) is summed to the input voltage, which is then converted to a current by *A1(s)*: this is a transconductance amplifier with an high frequency pole to reduce noise. The current at the output of *A1(s)* is sent to *OT*, converted to a light; this light is then sent to *OR1* and reconverted to a current. Nevertheless, as it has been shown in section II, *OT* has a transmitted light power which has not a linear relationship with the input current. Therefore another optical receiver, *OR2*, matched with *OR1*, is used. It receives the light signal, coming from *OT*, and converts it in a current, converted then in a voltage by *A2(s)*; this is a transresistance amplifier with an high frequency pole to reduce noise. The output of *A2(s)* is used to make a feedback on the light power transmitted by *OT*: in such a way the relationship among the voltage at the input of insulation stage and the current at its output is linearized. The output current of *OR1* is sent to *A3(s)*, a transresistance amplifier with an high frequency pole to reduce noise. Another active component is at the transducer output: it is used to adjust gain and offset of output voltage. Offset voltages and variable gains used in the circuit are obtained, respectively, by means of voltage regulators and resistive trimmers.

Another important parameter is the power supply of the electronic components of the circuit; in order to preserve insulation realized with *OT*, *OR1* and *OR2*, two separated power supplies have to be used. They are obtained by means of two DC/DC converters, which guarantee insulation up to 5000 V_{RMS}.

On the whole, the transducer is designed to have input range of ±1200 V, output range of ±5 V and insulation of 5000 V_{RMS}. It is composed of only low cost components.

4 Simulations of the transducer

The RVT has been simulated in PSpice environment. Simulations have been used to aid the design of the RVT. Models of the real electronic components, developed by producers, have been used to simulate the RVT. As it has been said before, the RVT is thought to have accuracy of ±0.1 % at least in the frequency range of DC-9 kHz. Important design constraints are the maximum current of 30 mA in the OT, and its maximum reverse voltage 9 V. Another design parameter is the minimum value of current: as it is shown in section II, choosing 1 mA, the RVT will operate in the region of maximum linearity for the optical insulation stage. Therefore the values of resistances and capacitances have been chosen to fulfil these constraints and goals.

Simulations in time and frequency domains have been made and in the following some results are reported. Figures 6 and 7 show results of the simulation made with maximum input voltage, i.e. ±1200 V, and frequency of 50 Hz. The first of them shows input and output voltages, where output voltage is multiplied by the rated ratio of 240. It can be seen that the two waveforms are practically overlapped. Figure 7 displays current in the OT: its lowest value is about 1 mA and its peak value is about 29 mA. It is worthwhile noting that this is an anomalous operating condition, since the rated voltages are about ±325 V or ±565 V, depending on the measured signal if it is line to neutral or line to line. If input voltage is line to neutral, then OT current is in the range of 11÷19 mA, while if it is line to line, OT current is in the range of 8÷22 mA.

In Figure 8 there are the results of a frequency domain simulation: it displays the ratio between the output voltage, multiplied by the rated ratio of 240, and the input voltage, at its maximum value of ±1200 V. It is clear that it is one at low frequencies and at 100 kHz it decreases of about 0.2 %. At 9 kHz it decreases less than 0.01 %.
From simulations it can be gathered that the RVT has a performance better than that prescribed by [2].

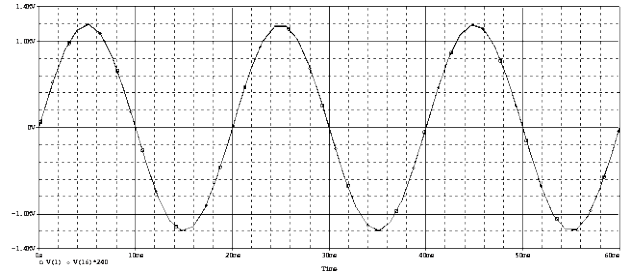

Fig. 6 - Maximum input voltage and output voltage, multiplied by rated ratio, at frequency of 50 Hz.

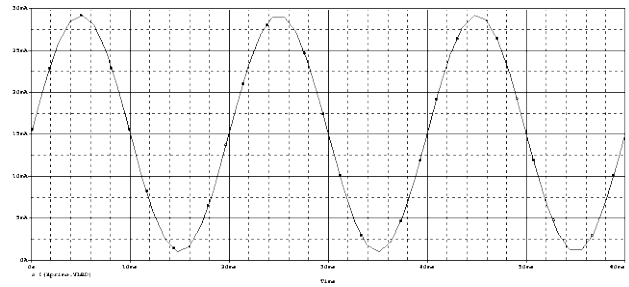

Fig.7 - Current in the optical transmitter, at maximum input voltage and frequency of 50 Hz.

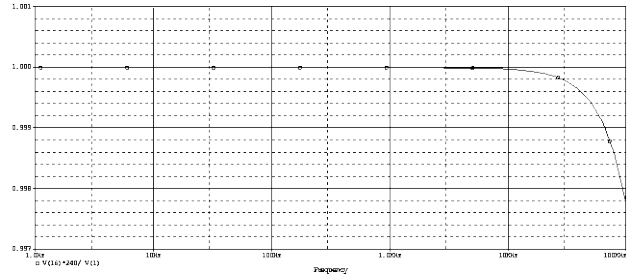

Fig.8 - Frequency bandwidth of the realized voltage transducer

5 Characterization of the Transducer

After that the RVT has been simulated, a prototype has been realized. The first version has been built on a bread board, to prove that real operation was similar to that simulated, and then a PCB has been realized. In order to characterize the prototype of the RVT an automated measuring station (AMS) has been set up. Then some experimental tests have been carried out. In the following subsections the descriptions of the AMS and of the experimental tests will be presented.

5.1 The Automated Measuring Station

The block scheme of the AMS ([18]) is shown in Figure 9. It is divided in two sections: a control and a power section.
The control section is based on a PXI platform, which comprehends a controller, a function generation module (FG) and a data acquisition module (DAQ). FG has an analog output at 16 bit, ±12 V output range, 100 MHz maximum generation frequency and a memory of 256 MB. DAQ has 8 synchronous analog inputs at 14 bits, ±10 V input range and 2.5 MHz maximum simultaneous sampling rate per channel.

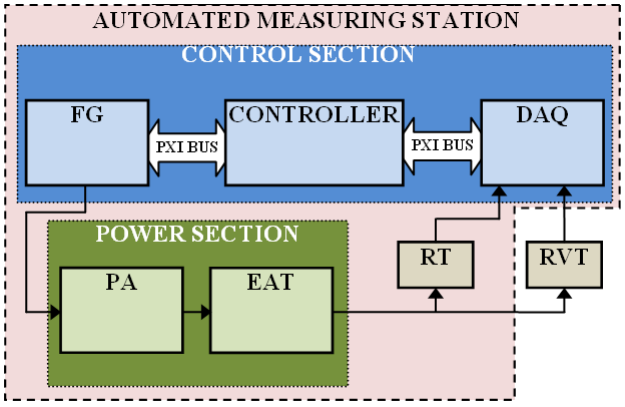

Fig. 9 - Block scheme of the automated measuring station.

The power section consists of a power amplifier (PA) and an elevator autotransformer (EAT). The utilized power amplifier is the Kepco 15-20M, with output ranges of $\pm 15\ V_{peak}$ for voltage and $\pm 20\ A_{peak}$ for current; used as voltage amplifier, its frequency bandwidth is in the range of DC-300 kHz with unity gain. As elevator autotransformer the Kepco ATB 15-200 has been employed: its input is in the range of $\pm 15\ V_{peak}$, its output in the range of $\pm 360\ V_{peak}$ and the output power is 200 W. The AMS includes, furthermore, a resistive divider, with accuracy of 0.01 %, as reference transducer (RT). By means of FG, the desired waveforms are generated in the range of ±12 V; PA is used as preamplifier, to supply enough power to drive EAT. At the output of EAT voltage waveforms are in the range of $\pm 360\ V_{peak}$. EAT output is transduced by RT and RVT and their outputs are simultaneously sampled by DAQ, with a sampling frequency which is an integer multiple of the frequency of the

generated signal. Measurement software has been developed in LabWindows/CVI, a C programming environment, measuring instruments oriented, distributed by National Instruments.
The first test is finalized to verify the performance of the control section of the AMS. Sinusoidal waveforms with amplitude of 10 V_{peak}, frequency variable in the range of 10 ÷ 100000 Hz have been generated. Figure 10 show ratio error and phase displacement of the AMS, evaluated with the formulas (1) and (2) explained in the next subsection. Maximum deviations in amplitude and phase are lower than, respectively, 15 p.p.m. and 1 mrad.

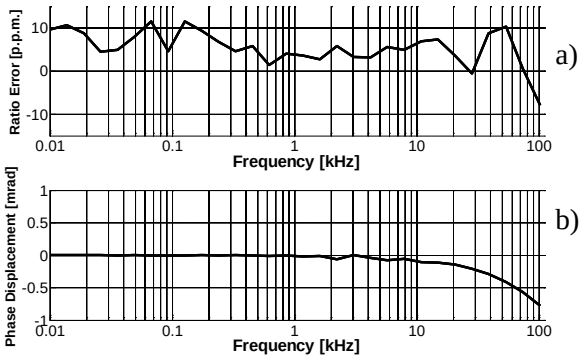

Fig. 10 - Ratio error and phase displacement of the control section of the AMS.

5.2 Ratio error and phase displacement

The first group of tests on RVT has been performed in order to characterize its operation in terms of ratio error and phase displacement. Sinusoidal voltages have been generated: the amplitude has been kept constant to 230 V_{RMS} while fifty frequency values, logarithmically spaced, have been chosen in the range of 10-100000 Hz. Each test has been repeated ten times. For each test, ratio error and phase displacement have been measured, respectively, as in (1) and (2), extending their definitions reported in [19] in order to account other frequency points than fundamental component.

$$\Delta R(f_k) = 100\left(\frac{R_{R,RVT}\cdot V_{RVT}(f_k) - R_{R,RT}\cdot V_{RT}(f_k)}{R_{R,RT}\cdot V_{RT}(f_k)}\right) \quad (1)$$

$$\Delta\varphi(f_k) = \varphi_{RVT}(f_k) - \varphi_{RT}(f_k) \quad (2)$$

In (1), $R_{R,RVT}$ and $R_{R,RT}$ are the rated ratios, respectively, of the RVT and of the RT; $V_{RVT}(f_k)$ and $V_{RT}(f_k)$ are, respectively, r.m.s. values of the output voltages of the RVT and of the RT when frequency of input voltage is f_k.
In (2), $\varphi_{RVT}(f_k)$ and $\varphi_{RT}(f_k)$ are the phase angles of the fundamental components of the output of the RVT and of the RT, respectively. Figure 11 shows ratio error of the RVT, together with the accuracy range. This range has been obtained as ±3σ, with σ the standard deviation evaluated on the ten iterations of each test. It can be seen that until 9 kHz accuracy range is in the interval of ±0.07 %, better than it is prescribed by [2], until 100 kHz it is in the interval of ±0.1 %.
Similarly to Figure 11, Figure 12 displays phase displacement of the RVT together with the accuracy range. It can be gathered that phase displacement is about -40 mrad at 9 kHz and it is lower, as absolute value, than -300 mrad at 100 kHz.
From the first group of tests RVT results to have performance better than that prescribed by [2].

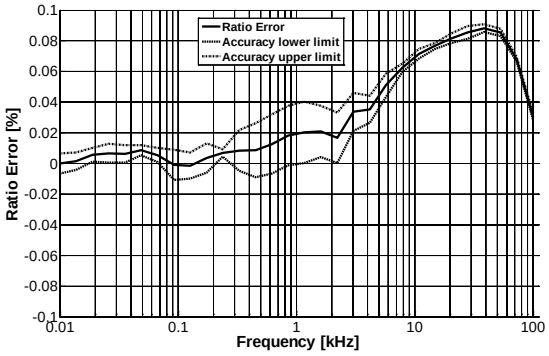

Fig.11 - Ratio error, with the accuracy range, of the realized voltage transducer.

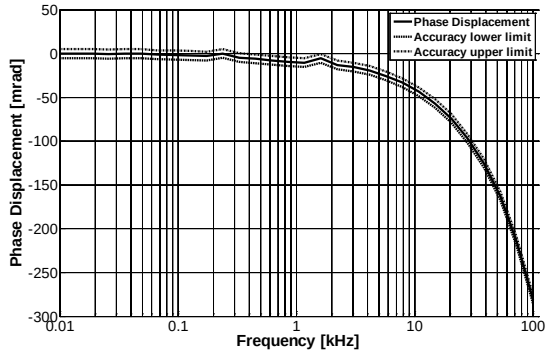

Fig. 12 – Phase displacement, with the accuracy range, of the realized voltage transducer.

5.3 Linearity and distortion tests

The second group of tests has been performed in order to characterize the linearity and the distortion of the RVT.

In a first test, static linearity has been verified. An increasing ramp with amplitude of $\pm 5\ V_{peak}$ and frequency of 1 Hz has been supplied at input of the insulation stage of the RVT, where the full scale (F.S.) range is ±5 V, thus excluding the input stage. A linear fitting of the output values of the RVT has been executed and in Figure 13 the root mean square error (RMSE), expressed as percentage of F.S., as function of RVT input, is shown. It can be seen that the maximum RMSE is 0.06 %.

In the second test, dynamic linearity has been verified. Sinusoidal waveforms have been generated: ten amplitude values in the range of $23 \div 230\ V_{RMS}$ and two frequencies of 50 Hz and 10 kHz have been chosen. In all the tests, r.m.s. of the output of the transducer has been calculated and multiplied for the rated ratio; then a linear fitting has been executed. Figure 14.a and Figure 14.b show RMSE of the linear fitting, expressed as percentage of F.S., as function of RVT input normalized to $230\ V_{RMS}$, respectively at frequency of 50 Hz and 10 kHz. Maximum RMSE is 0.003 % of F.S. range.

In the third and the fourth group of tests the distortion of the RVT has been verified. Sinusoidal waveforms have been generated: in the third the amplitude has been kept constant at $230\ V_{RMS}$ and frequency has been varied in the range of 30-100000 Hz; in the fourth, amplitude has been varied in the range of $23 \div 230\ V_{RMS}$ and two frequencies of 50 Hz and 10 kHz have been chosen. In all the tests total harmonic distortion (THD) of the output of the RVT has been evaluated: in the third group one hundred harmonic components have been measured, while in the fourth one thousand. Figure 15 shows the THD as function of frequency, in the third group of tests; Figure 16.a and Figure 16.b show the THD as function of RVT input amplitude normalized to $230\ V_{RMS}$. The maximum THD value is 0.08 %; anyway, in the typical operating conditions, i.e. frequency of 50 Hz and amplitude of $230\ V_{RMS}$, its value is under 0.04 %.

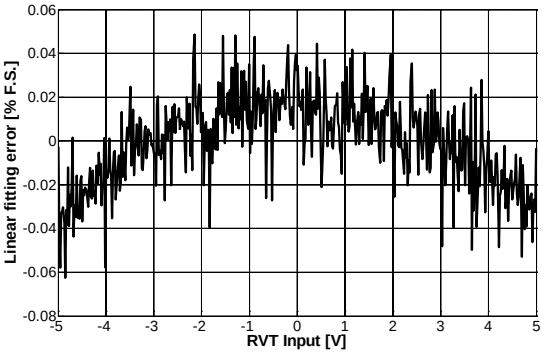

Fig. 13 - Root mean square error of the linear fitting as function of RVT input, in the static linearity test.

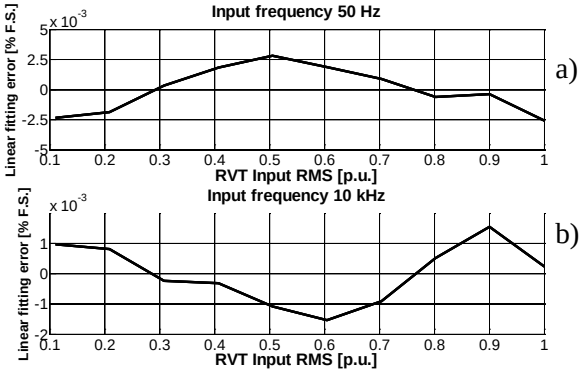

Fig. 14 - Root mean square error of the linear fitting as function of RVT input, in the dynamic linearity test at frequencies of 50 Hz (a) and 10 kHz (b).

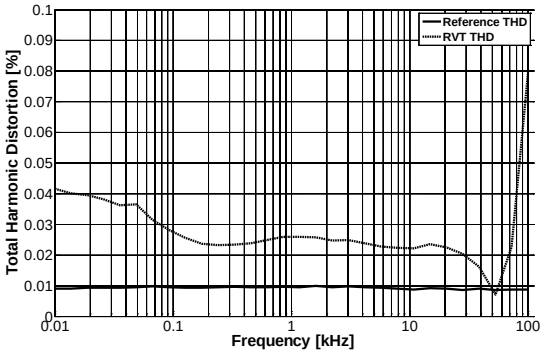

Fig. 15 - Total harmonic distortion of the RVT as function of the frequency.

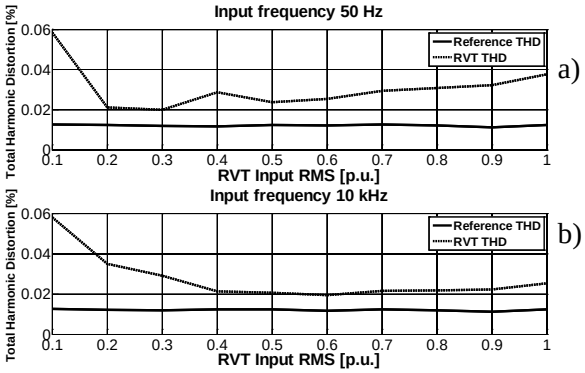

Fig. 16 - Total harmonic distortion of the RVT as function of RVT input amplitude, at frequencies of 50 Hz (a) and 10 kHz (b).

5.4 Tests in distorted operating conditions

In this last group of tests the performance of the RVT in distorted operating conditions has been evaluated.

For the first test of the group, a distorted voltage waveform of a non linear circuit is taken from IEEE standard 1459 [20]. Fundamental frequency is 50 Hz and r.m.s. of fundamental component is 230 V.

Relative amplitudes and phase angles of harmonic components are detailed in Table 1.
For the second and the third test of the group, waveforms taken from [21] have been used. In particular, the second test is aimed to confirm effectiveness of RVT at frequencies lower than industrial frequency: therefore, voltage waveform presenting interharmonics has been used. Fundamental frequency is 50 Hz and r.m.s. of fundamental component is 230 V. Two interharmonic components have been added to fundamental tone: they have frequencies of 5 and 25 Hz, amplitudes of 5 % of fundamental tone and zero phase.
The third test is aimed to confirm effectiveness of RVT at frequencies higher than industrial frequency. Therefore, voltage waveform presenting high order harmonics has been used. Fundamental frequency is 50 Hz and r.m.s. of fundamental component is 230 V. Five harmonic components have been added to fundamental tone: their parameters are shown in Table 2.

Table 1. Parameters of the waveform used in the first test in distorted conditions.

Harmonic order	Amplitude [% fundamental component]	Phase angle [deg]
1	100	-0.74
3	10.28	6.76
5	4.92	142.30
7	7.44	146.70
9	8.64	-47.40

Table 2. Parameters of the waveform used in the third test in distorted conditions.

Harmonic frequency [Hz]	Amplitude [% fundamental component]	Phase angle [rad]
5000	30	0
10000	25	0
20000	20	0
30000	15	0
40000	10	0

Figures 17.a, 18.a and 19.a show input and output of the RVT, with amplitudes normalized to maximum value of the input signal and with the output multiplied by the rated ratio of the RVT, for the three tests described above.
Figures 17.b, 18.b and 19.b show the difference among the curves in Figures 17.a, 18.a and 19.a. For these three tests, r.m.s. of error curves shown in Figures 17.b, 18.b and 19.b, are respectively 0.20 %, 0.22 % and 1.2 % of the r.m.s. of the curves in Figures 17.a, 18.a and 19.a.
It is worthwhile noting that these kind of indices include the effect of both ratio error and phase displacement of the RVT.

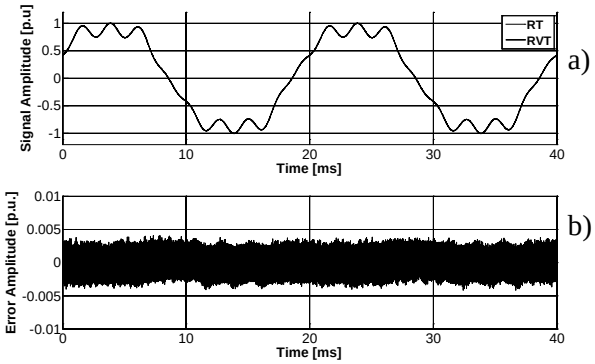

Fig. 17 - Test in distorted conditions: fundamental and harmonic components.

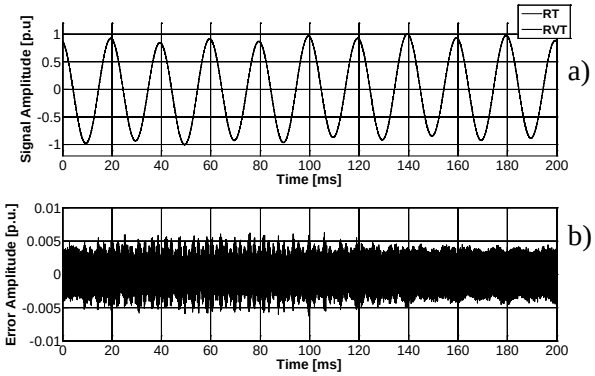

Fig. 18 - Test in distorted conditions: fundamental component and two interharmonics at 5 and 25 Hz.

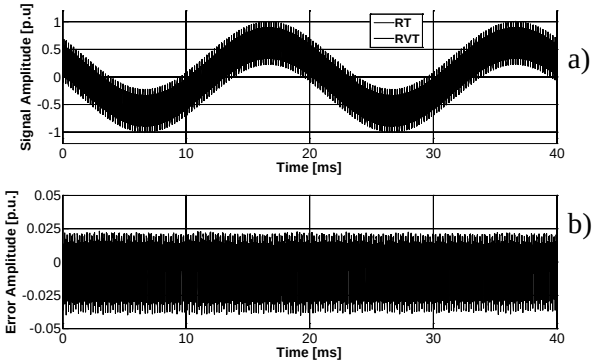

Fig. 19 - Test in distorted conditions: fundamental component and high order harmonics.

From this group of tests it is clear that RVT exhibits very good performance in typical situations of power systems, as it is that in test one. Anyway, also in extreme conditions, with very strongly deformed waveforms, as it is that in test three, it exhibits good performance.

6 Conclusion

In this paper a method for linearization of optically insulated voltage transducers is presented. It makes possible to realize voltage transducers, for power system applications, with high performance. The method has been applied to the design and implementation of a low cost optically insulated voltage transducer. The dimensions of the prototype are 8x8x4 cm^3 and its cost is about 30 €. Several tests have been performed to characterize transducer operation: ratio error, phase displacement and THD are lower than, respectively, 0.1 %, 300 mrad and 0.08 % until 100 kHz; non-linearity error is lower than 0.06 %. Moreover, tests in distorted operating conditions have been carried out: even in extreme situations, with strongly deformed waveforms, the transducer exhibits very good performance. The high performance and the low cost of the realized transducer prove the effectiveness of the presented linearization method.

References:

[1] IEC EN 50160, "Voltage characteristics of electricity supplied by public distribution systems", 03/2000.

[2] IEC EN 61000-2-4: "Environment - Compatibility levels in industrial plants for low-frequency conducted disturbances", 04/2003.

[3] IEC EN 61000-4-30: "Testing and measurement techniques – Power quality measurement methods", 11/2003.

[4] G. Bucci, E.Fiorucci, A. Ometto, N. Rotondale " The Voltage Amplitude Modulations and Their Effects on Induction Motors" *WSEAS Transactions on POWER SYSTEMS*, issue 2, volume 1, february 2006, pages 488-496 ISSN: 1790-5060

[5] E. Fiorucci, G. Bucci, F. Ciancetta, "Metrological Characterization of Power Quality Measurement Stations: a Case Study" *IJIT International Journal of Instrumentation Technology (IJIT)* ISSN: 2043-7862 DOI 10.1504/IJIT.2011.043595

[6] D. Castaldo, D. Gallo, C. Landi, E. Fiorucci "Measurement Network Infrastructure for Power Quality Monitoring" *Shaker Verlag Transactions on Systems, Signals and Devices*, volume 1, no. 4, pp. 387-404, 2005-2006. ISSN: 1861-5252

[7] Kawamura, K.; Saito, H.; Noto, F.; "Development of a high voltage sensor using a piezoelectric transducer and a strain gage", *Instrumentation and Measurement, IEEE Transactions on*, Volume: 37 , Issue: 4, Publication Year: 1988 , Page(s): 564 – 568

[8] Aikawa, E.; Ueda, A.; Watanabe, M.; Takahashi, H.; Imataki, M.; "Development of new concept optical zero-sequence current/voltage transducers for distribution network", *IEEE Trans. On Power Delivery*, Vol. 6, Issue 1, Jan. 1991 Page(s):414 – 420

[9] L. H. Christensen, "Design, construction, and test of a passive optical prototype high voltage instrument transformer," *IEEE Trans. Power Delivery*, vol. 10, pp. 1332–1337, July 1995.

[10] Fam, W.Z.; "A novel transducer to replace current and voltage transformers in high-voltage measurements", *Instrumentation and Measurement, IEEE Transactions on*, Volume: 45 , Issue: 1, Publication Year: 1996 , Page(s): 190 – 194

[11] Cruden, A.; Richardson, Z.J.; McDonald, J.R.; Andonovic, I.; Laycock, W.; Bennett, A.; "Compact 132 kV combined optical voltage and current measurement system" *Instrumentation and Measurement, IEEE Transactions on*, Volume 47, Issue 1, Feb. 1998 Page(s):219 – 223

[12] C. Svelto, R. Ottoboni, A. M. Ferrero, "Optically-supplied voltage transducer for distorted signals in high-voltage systems", *Instrumentation and Measurement, IEEE Transactions on* Vol. 49, Issue 3, June 2000 Page(s):550 – 554.

[13] Rahmatian, F.; Chavez, P.P.; Jaeger, N.A.F.; "230 kV optical voltage transducers using multiple electric field sensors", *Power Delivery, IEEE Transactions on*, Volume 17, Issue 2, April 2002 Page(s):417 - 422

[14] P. Niewczas, L. Dziuda, G. Fusiek, J. R. McDonald; "Temperature Compensation for a Piezoelectric Fiber-Optic Voltage Sensor", . *Proceedings of IEEE Instrumentation and Measurement Technology Conference, IMTC 2006* Page(s):1994-1998

[15] A. Delle Femine, C. Landi, M. Luiso, "Optically Insulated Low Cost Voltage Transducer for Power Quality Analyses", *Springer & Verlag Transactions on Systems, Signals and Devices* Vol. 4, No. 4, Issues on Sensors, Circuits & Instrumentation, December 2009

[16] A. Delle Femine, D. Gallo, C. Landi, M. Luiso, "Broadband Voltage Transducer with Optically Insulated Output for Power Quality Analyses", *Proceedings of IEEE Instrumentation and Measurement Technology Conference IMTC 2007*, 1-3 May 2007, Warsaw, Poland.

[17] Johnson, Mark; "*Photodetection and Measurement - Maximizing Performance in Optical Systems*", McGraw-Hill, 2003.
[18] Khalil, Hassan K.; "Nonlinear systems", (second edition), Prentice Hall, 1996.
[19] D. Gallo, C. Landi, M. Luiso, "A Voltage Transducer for Electrical Grid Disturbance Monitoring over a Wide Frequency Range", *Proceedings of IEEE International Instrumentation and Measurement Technology Conference I2MTC 2010*, Austin, Texas, USA, May 3-6 2010.
[20] "Instrument Transformers-Part 1: Current Transformers", IEC Std. 60044-1, 2000.
[21] IEEE Standard Definitions for the Measurement of Electric Power Quantities Under Sinusoidal, Nonsinusoidal, Balanced or Unbalanced Conditions, IEEE 1459, 2000.
[22] D. Gallo, C. Landi, M. Luiso, "Real Time Digital Compensation of Current Transformers over a Wide Frequency Range", *Instrumentation and Measurement, IEEE Transactions on*, Volume: 59 , Issue: 5, Publication Year: 2010 , Page(s): 1119 - 1126